

# Understanding relationships among micrometeorological variables using Ameriflux data

---

Gopal Penny

May 1, 2014

## 1 Introduction

Fluxes in the planetary boundary layer drive much of the environmental behavior throughout the globe. Both local and global water budgets are largely driven by gaseous transfer of water vapor into the atmosphere. Estimating the trajectory of average global atmospheric carbon concentrations requires a detailed understanding of the local fluxes of different vegetation types in different climates. Measuring and modeling these fluxes are therefore critical to understanding the trajectory of our global climate. These processes have implications in global warming, water scarcity, and extreme storm events. Unfortunately we currently are unable to make good estimates of these fluxes everywhere on the planet, largely because collecting environmental data is often time-consuming and expensive. Fluxes through the planetary boundary layer are particularly expensive to measure. For instance, flux towers cost tens of thousands of dollars for equipment, and must be maintained over time to provide satisfactory data. Other methods for estimating surface fluxes do not measure the fluxes themselves, but rely on simplified models to estimate fluxes. The flux-gradient method includes the assumption that turbulent transport is diffusive, ignoring the effect of non-local transport due to large eddies, as well as counter-gradient transport due to turbulent structure and placement of sensors. Other methods are based on coupling biological with physical processes (Penman-Monteith) or manipulating and parameterizing simple physical relationships among micro-meteorological variables (Priestley-Taylor). In many cases, parameterizing these models is done by simple rule of thumb or other modifications that make the equation more tractable. In equations based on the energy balance, ground heat flux ( $G$ ) is an unknown variable

and often parameterized as one tenth of net radiation ( $R_n$ ). In other cases, measuring net radiation is difficult if the canopy is tens of meters high and there is not a good method for installing a sensor above the canopy. Measuring global shortwave incoming radiation could be a reasonable substitute if there is a clear relationship between  $R_g$  and  $R_n$ . In this report, I review a number of variables affecting the energy balance and attempt to distinguish relationships between key sets of variables.

## 2 Methods

Data analysis being the key component of this work, data collection and aggregation was important. Ameriflux Level 2 data was downloaded from the Ameriflux network. Analysis focused on a cross-section of sites with various climates and vegetation types. The primary sites included in this analysis were Chestnut Ridge (TN), Kendall Grassland (AZ), Mead Rainfed (), and NC Loblolly Pine (NC). Additional sites included Tonzi Ranch (CA), Duke Hardwood Forest (NC), and Santa Rita Mesquite Savanna (AZ). Each of these flux towers have been operated for a number of years, collecting a variety of data. Given the large variability at sub-daily timescales, data were averaged from sub-hourly timescales to the daily timescale. In order to avoid challenges with estimating nighttime fluxes (increase of the flux tower footprint, stable boundary layer, and variable turbulent structures), nighttime measurements were excluded from the averages. From here on, daily averages will refer to the daytime averages with nighttime values removed. Daytime was defined simply as periods where net radiation was greater than zero. This simplistic definition is valid most of the time, as net radiation is positive when the sun is shining.

Normalized Difference Vegetation Index was used as an index of green vegetation. Because Ameriflux generally does not calculate this index, NDVI data were obtained from MODIS products. Ameriflux webpages link to MODIS products corresponding to their sites. Gridded timeseries of satellite data is provided online, and aggregated at 16-day intervals. This data was downloaded and assimilated with the Ameriflux data. Additionally, NDVI was linearly interpolated between the 16-day averages to provide a daily estimate of NDVI at each of the sites.

Most of the analysis was done using ggplot in R, and visually interpreting plotted data. I include and describe these plots in the results section.

## 3 Results

### 3.1 Net radiation and global shortwave radiation

For the majority of the analysis, four sites were selected to cover a range of vegetation types including deciduous forest (Chestnut Ridge, TN), grassland (Kendall Grassland, AZ), agricultural crops (Mead Rainfed, XXXXXXXX), and coniferous forest (Loblolly Pine, NC). In order to obtain a basic understanding of the many processes affecting energy and mass fluxes, I first plotted timeseries of energy fluxes and soil moisture for 2006 (Figure 1) to see the trends throughout the year for a number of sites. These plots served as a sense check on the next pieces of analysis. They also illustrate some important relationships. For instance, the grassland is generally more dry with

higher sensible heat fluxes than the other land covers. The crops have a very high latent heat flux during growing season and low latent heat flux the rest of the year, while the forests have a gradual increase and decline of latent heat flux. While the maximum  $R_g$  is similar in at all sites through out the year, the grassland does not experience many days with low  $R_g$  suggesting fewer cloudy or rainy days. The soil heat flux is very low and constant in the forested sites, and higher and more variable at the other sites.

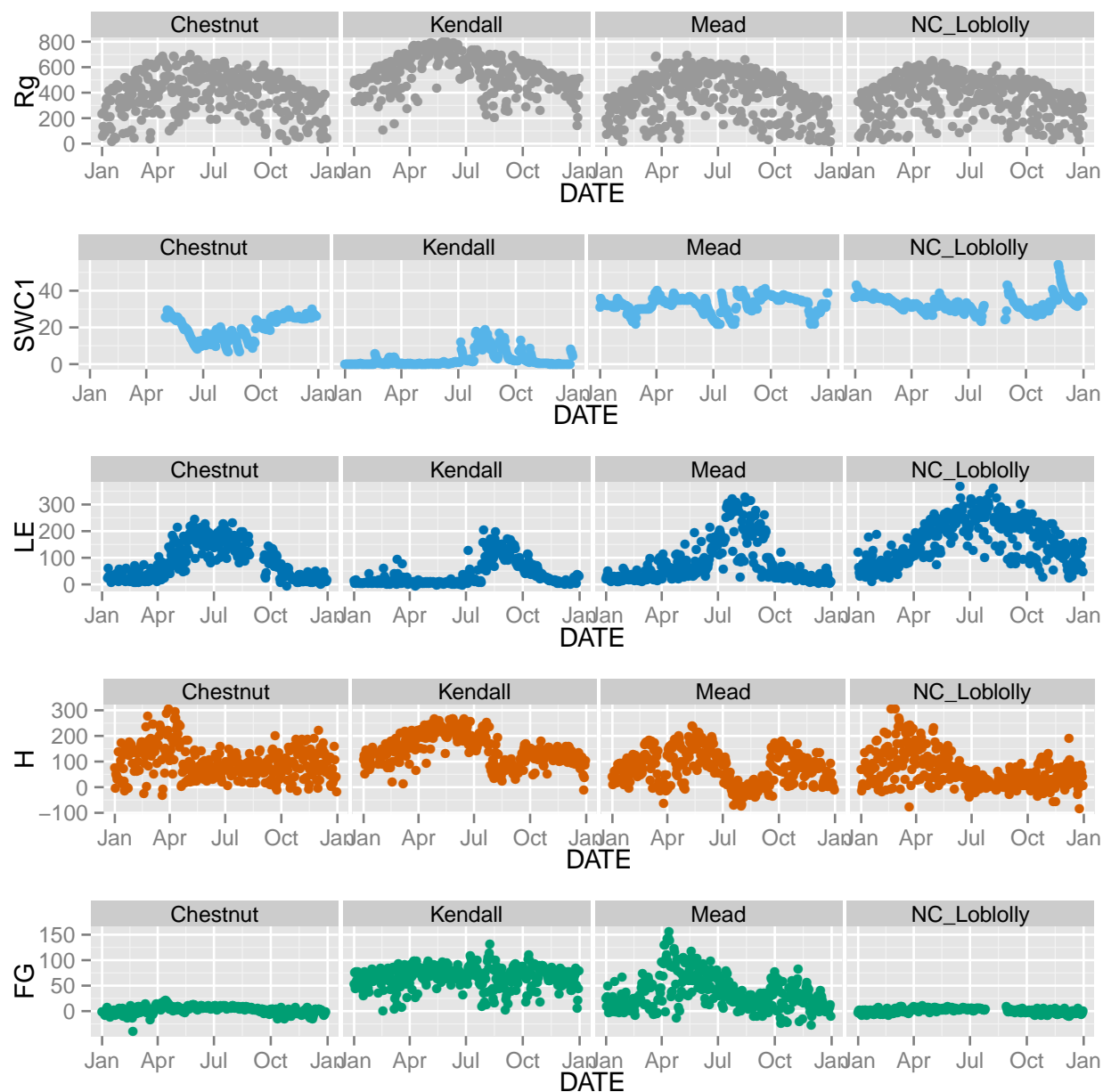


Figure 1: Daily timeseries of (a) net radiation, (b) surface water content, (c) latent heat, and (d) soil heat flux in 2006 at four Ameriflux sites.

Figure 2 shows energy fluxes normalized by net radiation, as well as the annual relationship  $R_n/R_g$ . The relationships among the energy fluxes are very apparent in this figure. The daily time-series is plotted in the top portion, while a smoothed average time series is plotted in the middle portion. At all sites except the grassland, latent heat is greater than sensible heat during growing season. The soil heat flux is high at the non-forested sites (up to 25% as expected  $R_n/R_g$  peaks when the land surface is cool, because a lower surface temperature results in reduced outgoing longwave radiation and increased net radiation for a given  $R_g$ ). However, the seasonal peak of  $R_n/R_g$  occurs before the seasonal peak of latent heat, suggesting other factors are at play. In the bottom plot, net ecosystem exchange (NEE) is color coded into the plot (NEE was not available for Chestnut Ridge). Maximum  $R_n/R_g$  clearly coincides with the minimum (most negative) NEE, the time when plants are growing fastest. It is possible that photosynthesis contributes as an additional energy sink and is the factor that pushes  $R_n/R_g$  to its peak.

In Figure 3,  $R_n$  is plotted over  $R_g$  for the full 2006 year, using daily (daytime) values. First, there is significant spread in Kendall Grasslands and Mead Rainfed agriculture, more so than the forest sites. This likely has to do with the forest sites retaining moisture and biomass throughout the year, while the other sites go through more drastic changes in soil moisture. The other point to note is that  $R_n/R_g$  is strongly correlated with soil moisture. Greater soil moisture likely leads to increased latent heat and soil heat fluxes, increasing  $R_n$ . To look at the relationship between  $R_n$  and  $R_g$  more closely, I plotted  $R_n/R_g$  versus surface water content (SWC1) using daily values from the growing season only, considerably reducing the variability in  $R_n/R_g$  at all sites. To obtain an upper bound estimate, I took the 0.8 quantile of  $R_n/R_g$ , and plotted this as the slope of a line through zero on  $R_n$  versus  $R_g$  plot, again containing only daytime fluxes from growing season. In this plot, the spread is largely eliminated. I included latent heat in the color of this plot. The points furthest from the line tend to have low latent heat, entailing a shift towards a maximum  $R_n/R_g$  ratio when LE is high. Lastly, I wanted to see if biomass production had an effect on the  $R_n/R_g$  relationship. The last plot in Figure 3 shows a small negative correlation between  $R_n/R_g$  and NEE in the grassland and agriculture, but a small positive correlation in the forest. I have not been able to think of a mechanism to describe these relationships.

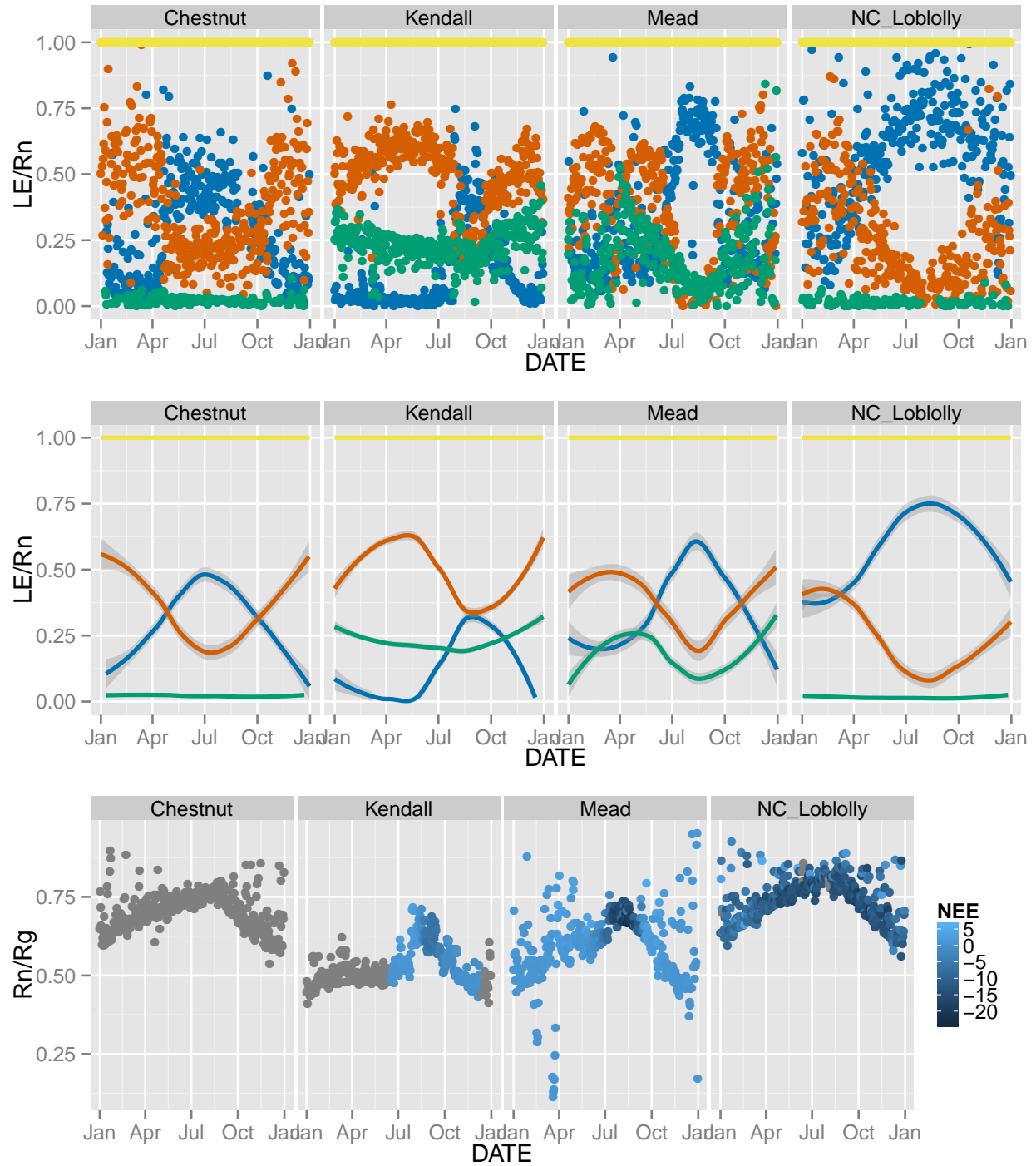


Figure 2: Normalized energy fluxes and  $R_n/R_g$  daily timeseries in 2006. (a) Normalized energy fluxes in 2006, (b) Normalized and smoothed energy fluxes in 2006, (c)  $R_n/R_g$  timeseries in 2006, with net ecosystem exchange (NEE) plotted in color.  $R_n/R_g$  generally reaches a maximum when NEE is greatest (most negative) due to plant carbon uptake.

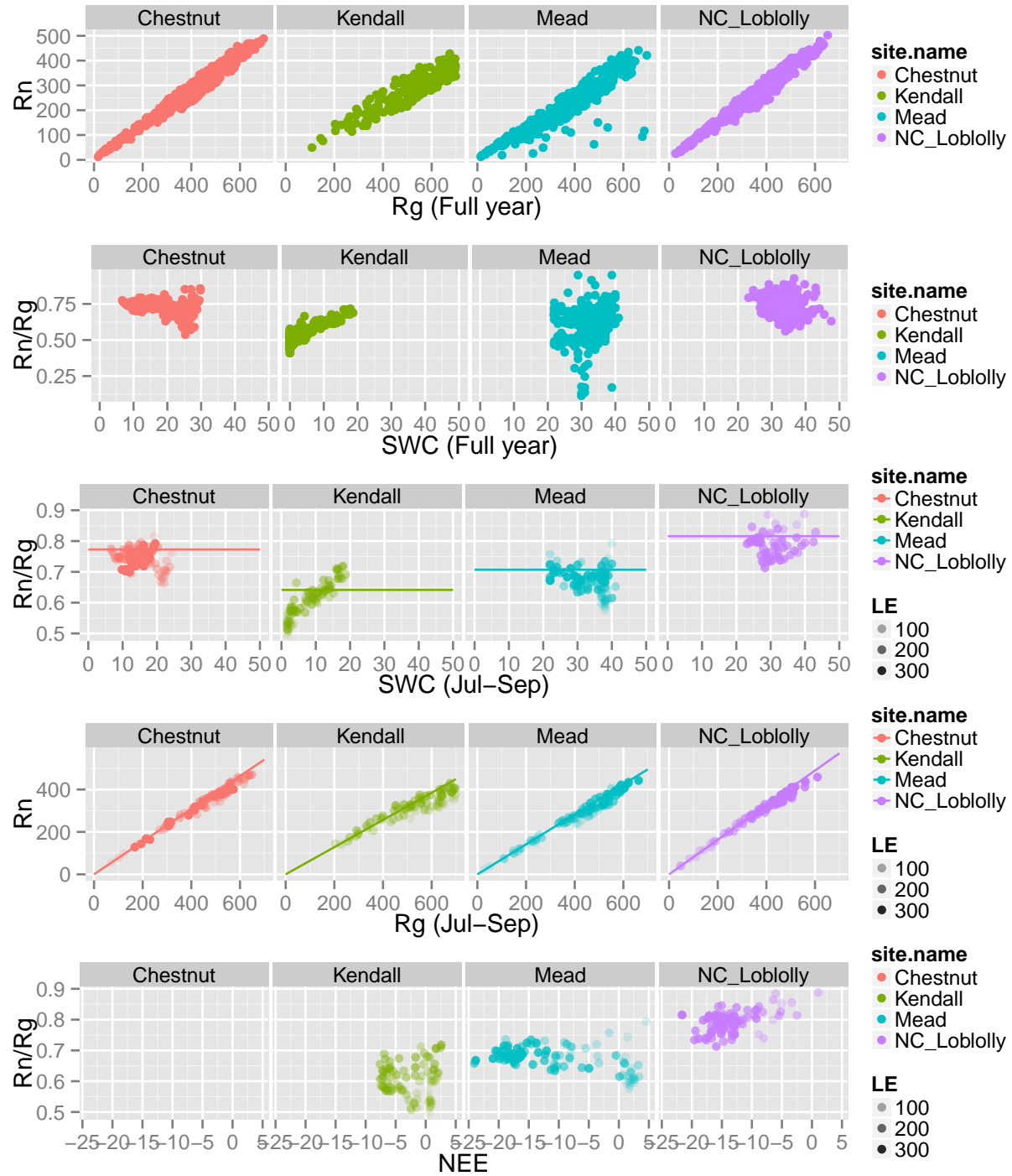


Figure 3: Relationships between  $R_n$ ,  $R_g$ , and SWC in the full year and growing season. (a)  $R_n$  vs  $R_g$  for 2006. (b)  $R_n/R_g$  vs soil water content in 2006. (c)  $R_n/R_g$  vs soil water content for the approximate growing season in 2006. The 0.8 quantile is plotted as an approximate envelope for this relationship. This value is the slope of the line in (d). (d)  $R_n$  vs  $R_g$  for approximate growing season in 2006, with the approximate envelope plotted as a line. The slope of the line is taken from (c).

### 3.2 Soil heat flux fraction and NDVI

The soil heat fraction is of importance to common evapotranspiration models, which often require net radiation ( $R_n$ ) and soil heat flux ( $G$ ) to be parameterized. In cases where data for  $G$  is unavailable, it is parameterized as a fraction of  $R_n$ , typically  $0.1 \times R_n$ . While this allows a first-order estimate to be calculated, it wholly ignores any changes in  $G$  with respect to  $R_n$ . In order to understand the relationship between these two variables better, I created a series of figures to understand how these fluxes change through out the year, and how they change with respect to each other and other variables. While soil moisture and other variables change considerably throughout the year, soil heat flux fraction ( $G/R_n$ ) is relatively constant. In forested catchments, it stays nearly-constant and close to zero, while in Kendall Grasslands and Mead Rainfed sites it varies more. There appears to be a local minimum when net carbon exchange (NEE) is at a maximum (on the plot it appears negative) for the non-forested sites. This peak coincides with the maximum NDVI (please note that the maximums on the plot are offset due to the legen shifting the NDVI plot to the left.

Further investigating the relationship between  $G/R_n$  and NDVI, I directly plotted the two against each other in Figure 5 using data from seven Ameriflux sites. This plot illustrates a number of points. There appears to be an upper envelope on the soil heat flux fraction which decreases with NDVI. In other words, as more lease collect sunlight, there is a small soil heat flux. Additionally, all the forested sites (shown in triangles) have a small soil heat flux fraction than the other sites. There are some negative fractions in this case, which mostly occur at very low net radiation, suggesting a winter value and a heat flux from the soil to the surface even during the day.

To separate the effects of vegetation type, I pulled all the forest sites and plotted them separately in Figure ??, and the non-forest sites below. The forest sites clump just above zero. The soil heat flux fraction appears to be uncorrelated with NDVI, net radiation, and soil water content in forested sites. The other sites, spanning grassland, agriculture, shrubs (savanna), and mixed woody savanna exhibit more complex behavior. All sites exhibit the upper envelop on  $G/R_n$ . Kendall grassland has low NDVI and low soil moisture throughout most of the year. Santa Rita mesquite savanna agriculture appears to have a small negative correlation between  $G/R_n$  and NDVI. Tonzi woody savanna exhibits no correlation between the two variables. As one might expect, the behavior of this mixed tree and grassland site is between the non-forest and forested sites. And lastly, Mead rainfed agriculture exhibit an upside-down "U" when examining the relationship between  $G/R_n$  and NDVI. It would appear that there is a positive correlation when  $R_n$  is small, and a negative correlation when  $R_n$  is large.

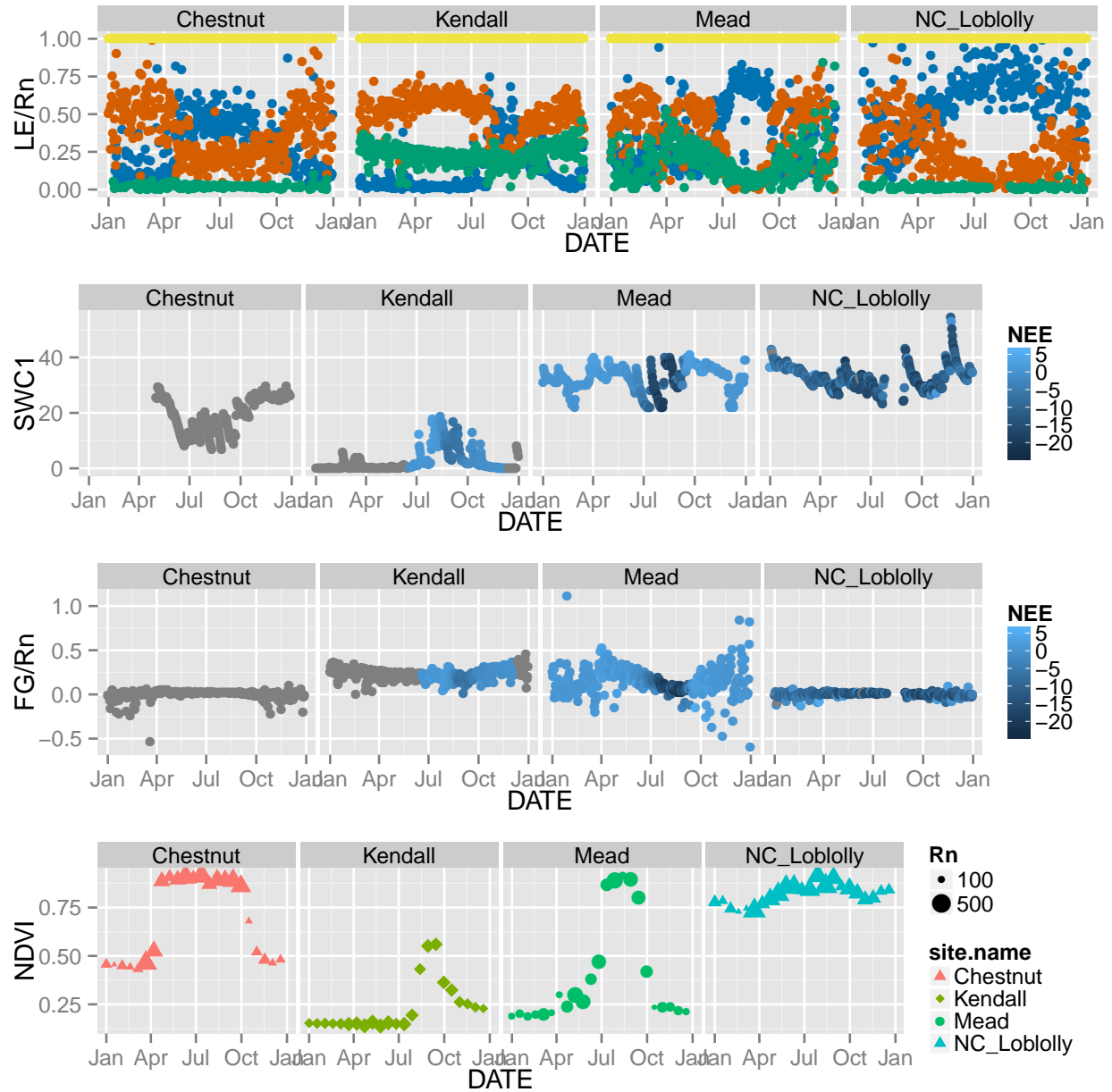


Figure 4: Timeseries variables illustrating relationships between vegetation and soil heat flux fraction in 2006 at four Ameriflux sites. (a) Daily energy balance fluxes including net radiation (yellow), latent heat (blue), sensible heat (orange), and soil heat flux (green). (b) Daily soil water content. (c) Daily soil heat flux fraction (soil heat flux divided by net radiation). (d) MODIS 16-day NDVI, with size and shape indicating net radiation and vegetation type, respective. Plotted for easy comparison with Figures X-XX.



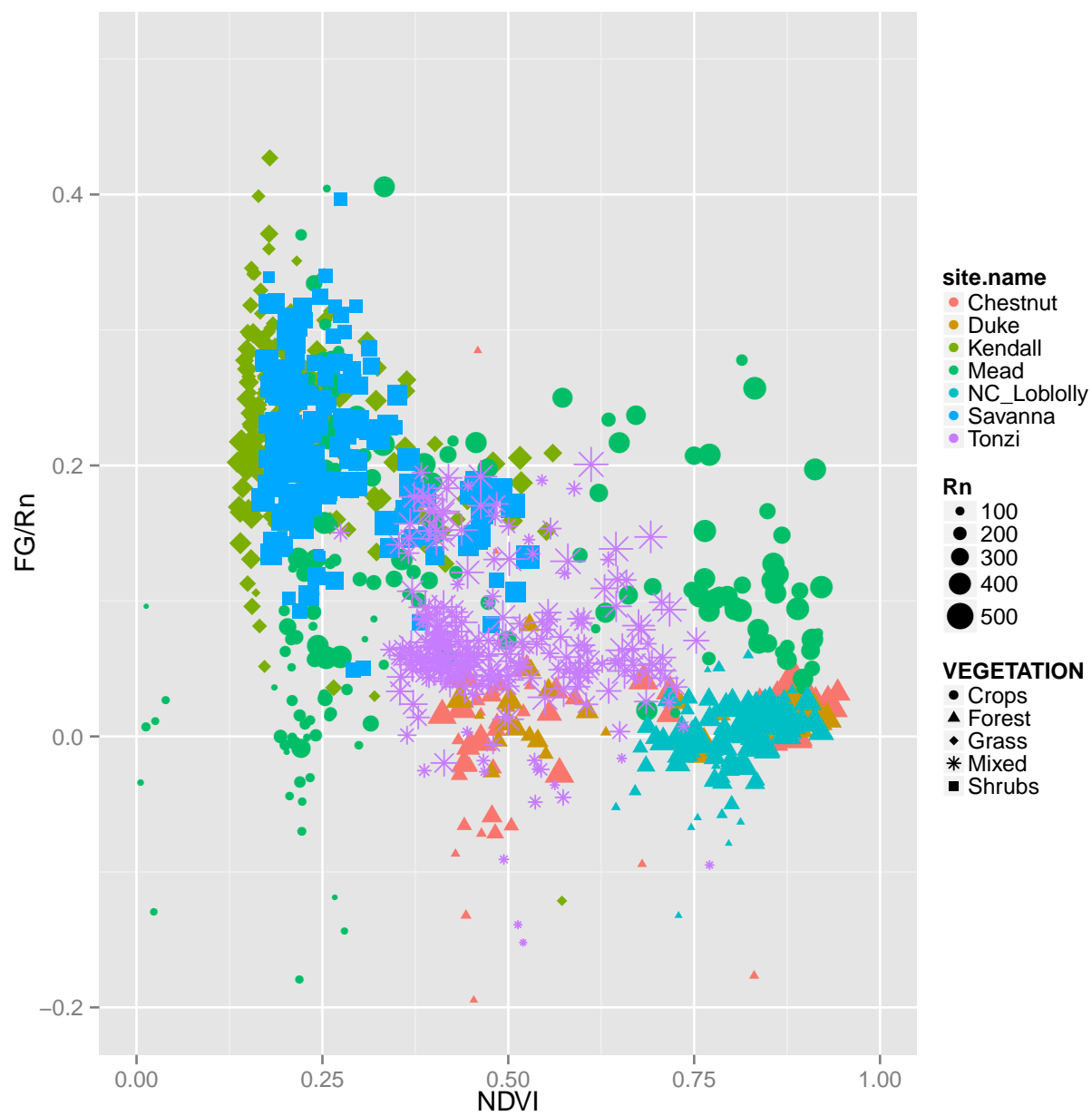


Figure 5:

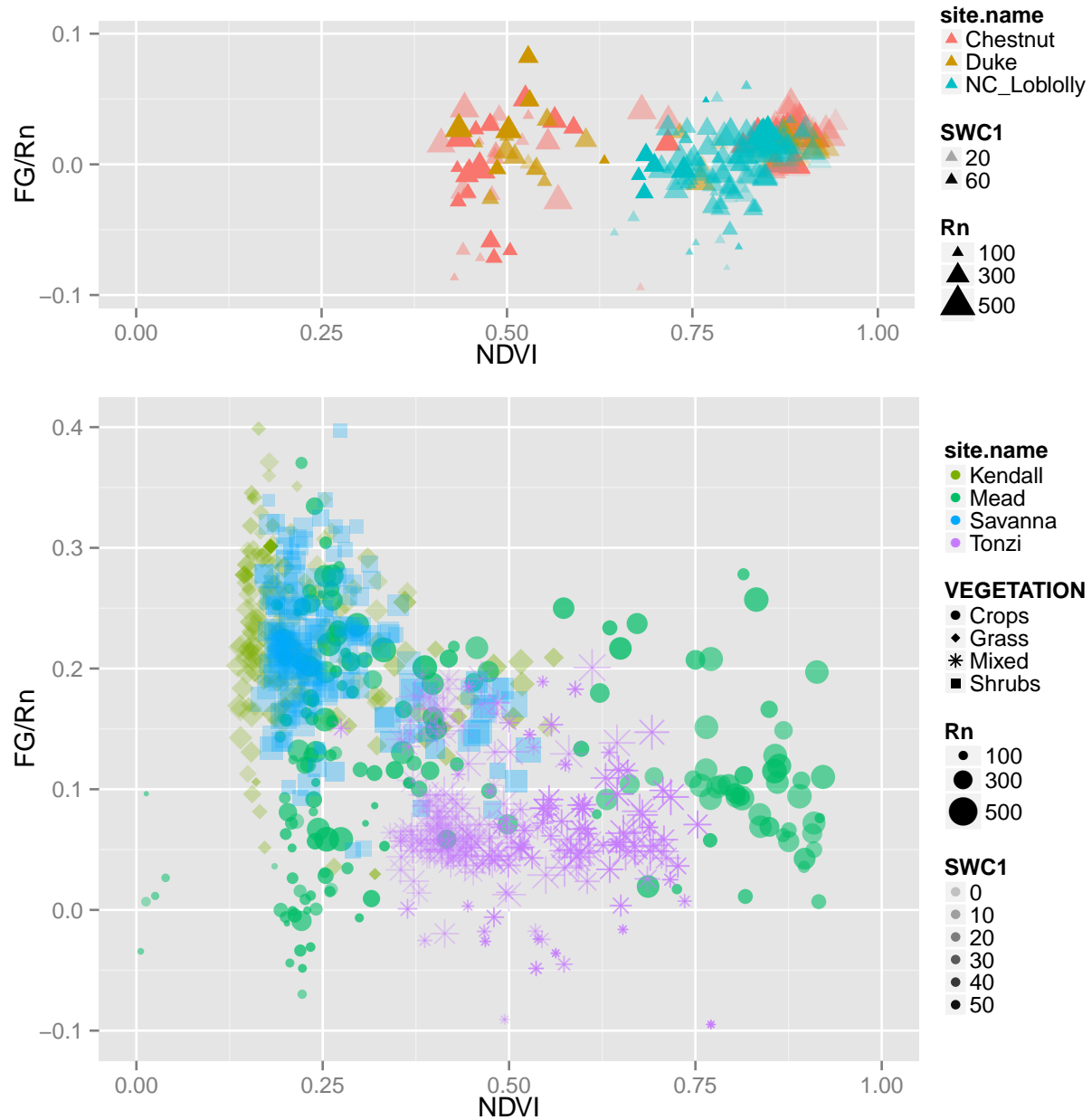


Figure 6:

## 4 Discussion and suggested future work

Make Rn vs Rg plots for multiple years. Time-average fluxes over 16-day period to match NDVI (reduce daily variations, utilize more data instead of just days that coincide with 16-day period). Note that the 16-day period was chosen to reduce the number of points in the figure which already overlap to some degree.